Influence of pressure on the crystallization of systems characterized by different intermolecular attraction

K. Koperwas,[1,2,*] F. Affouard,[3] J. Gerges,[3] L.-C. Valdes,[3] K. Adrjanowicz,[1,2] and M. Paluch[1,2]

[1]*Institute of Physics, University of Silesia, Uniwersytecka 4, 40-007 Katowice, Poland*

[2]*Silesian Center for Education and Interdisciplinary Research, 75 Pułku Piechoty 1a, 41-500 Chorzów, Poland*

[3]*Unité Matériaux et Transformations (UMET), Unités Mixtes de Recherche (UMR) Centre National de la Recherche Scientifique (CNRS) 8207, Unite de Formation et de Recherche (UFR) de Physique, Bâtiment P5, Université de Lille 1, 59655 Villeneuve d'Ascq, France*

(Received 27 September 2017; published 28 December 2017)

In this paper, we examine, in terms of the classical nucleation theory, how the strengthening of the attractive intermolecular interactions influences the crystallization process for systems like Lennard-Jones at different isobaric conditions. For this purpose, we modify the standard Lennard-Jones potential, and as a result, we obtain three different systems characterized by various strengths of attractive potentials occurring between molecules, which are in direct relationship to the physical quantities describing molecules, e.g., its polarizability or dipole moment. Based on performed analysis, we demonstrate that the molecular attraction primarily impacts the thermodynamics of the interface between liquid and crystal. This is reflected in the behavior of nucleation and overall crystallization rates during compression of the system.

DOI: 10.1103/PhysRevB.96.224106

I. INTRODUCTION

One of the main reasons for researchers' fascination with the transformation of a substance from the liquid into solid states is the possibility of occurrence of two different scenarios, i.e., liquid may form a regular arrangement of molecules of crystalline solids or a disorderly glassy state. Although, at first glance, the crystallization and the glass formation may seem to be two unconnected processes, in fact, they are closely related to each other because the glass can be formed only if the crystallization is inhibited enough. Thus, from the technological point of view, a crystallization impediment is a fundamental element for producing a glassy state; hence, quest of factors, which suppress creation of the crystal form within supercooled liquids, is of scientific interest [1–5].

Since a formation of an ordered phase (crystal) from the disordered liquid state is manifested by the discontinuous change in volume, the searching of the factors, which can facilitate or inhibit crystallization, has been initially focused on the thermodynamic aspects of this process. Considering a raise in the melting temperature T_m caused by increase in the pressure p and, related to it, gain in the driving force for crystallization process Δg, Tammann [6] and his student [7,8] put the primary emphasis on the favorable but only qualitative influence of p on the crystallization tendency. For the first time, the effect of the pressure on the thermodynamic driving force has been quantitatively estimated by Sirota [9], who related it to decrease in the energy barrier ΔW, which must be overcome to create the nucleus. Further studies suggested that the pressure also impacts the solid-liquid interfacial free energy γ [10], which affects ΔW. As in general, the nucleation barrier lowers with the pressure, it could be expected that a rise in the pressure causes lowering of γ, hence favors the crystallization (as is similar to the increase in Δg triggered by gain in p).

The above implies that from the thermodynamic point of view, the tendency of the material to crystallization should become higher at higher pressures. In other respects, the increase in pressure reduces the mobility of molecules, i.e., it causes the decrease in the diffusion, which makes that the time needed to form crystal become longer. Both thermodynamic and kinetic effects are included in the framework of the classical nucleation theory (CNT). At this point, note that in the critical case, the kinetic factor may even nullify, expected from the thermodynamic point of view, acceleration of the crystallization rate [10,11]. Therefore, the mutual interplay between thermodynamic and kinetic effects caused by the increase in the pressure determines the behavior of the overall crystallization process [12–15]. For example, some low-molecular weight glass-forming liquids exhibit suppression of the crystallization with compression [14,16], whereas in the case of polymers, extending of the degree of crystallinity is achievable by increasing of pressure [17,18]. These contrasting examples clearly show that our understanding of the influence of pressure on crystallization process is actually deficient and still requires further studies.

The effect of pressure on crystallization process can be studied experimentally in a very convenient way by using the broadband dielectric spectroscopy, which monitors reorientations of the dipole moment of the molecule μ. In this context, note that the value of the dipole moment influences mutual, attractive interactions between molecules and that its effect on the tendency to crystallization was studied in a recent paper [19]. Presented therein, experimental results suggest that substances, of which molecules possess a bigger value of μ, exhibit lower tendency to crystallization, i.e., they are better glass formers. The above conclusion has been likewise validated by the results from the computer simulations. Using CNT, it has been demonstrated that the optimal temperatures ranges for two main components of the overall crystallization process, i.e., nucleation rate and crystal growth rate, are more separated from each other for systems with the stronger intermolecular attraction. Separation of the nucleation and crystal growth processes impedes overall

*Corresponding author: kajetan.koperwas@smcebi.edu.pl

crystallization because the initial stage of crystallization, during which the crystal nucleus is formed (nucleation), is not sufficiently supported by the second process, during which the nucleus grows. Thus, the overall crystallization rate is limited, and then the glass formation becomes easier to achieve (at least) at studied constant isobaric conditions. However, possible separation of the nucleation and growth curves has not been studied in the context of discussed effect of the pressure on crystallization process. Consequently, a question that we would like to address is whether the pressure has the same effect on crystallization kinetics of systems that differ in strength of intermolecular attraction potential.

From the fundamental point of view, thermodynamics, dynamics, and structural properties of any kind of the real materials, e.g., van der Waals liquids, polymers, ceramics, and metallic alloys, are determined by the shape of molecules, their masses, and interaction potential $V(r)$. Then, the forces occurring between molecules also determine the crystallization tendency and the glass-forming ability. The intermolecular potential characteristics that favor crystallization seem to be a critical aspect of the crystallization process understanding. Unfortunately, investigations devoted to this problem cannot be easily performed using the traditional experimental methods because of structural complexity of real materials and difficulties in their explicit potential parameterization. However, these problems can be easily omitted using computer simulations, which enable the study of simple systems with a well-defined interaction potential at very wide ranges of pressures and temperatures (frequently not available in experiments). Also note that although there are not any reliable experimental methods for measuring the interfacial free energy at the boundary between liquid and crystal phases, γ can be determined at the melting point in computer simulations using three recently suggested methods: the cleaving potential method [20–22], the capillary fluctuation method (CFM) [23–26], and the Gibbs-Cahn integration technique [27,28]. Thereby, the use of molecular dynamic computer simulations opens up new opportunities in the investigations of homogeneous crystallization and applicability of CNT [29].

The first numerical molecular dynamic studies of crystallization were performed in the 1960s. Due to limited computer power, the explored systems were simple liquids, i.e., argonlike made of single atoms interacting by pairwise hard-sphere or Lennard-Jones (LJ) potentials [30]. Nevertheless, these simple systems relatively well reproduce properties of much more complex materials; in fact, more than 50 yr later, they are still of interest [31]. However, in recent decades, relatively few researchers have systematically studied the influence of changes in the interaction potential on glass-forming/crystallization ability [32–34]. In this context, note the studies of Berthier and Tarjus who compared the structures and the dynamics of a standard LJ glass-forming liquid mixture with and without the attractive tail of intermolecular potential [35]. The authors concluded that at temperatures characteristic of viscous liquid behavior, the dynamics of the system is strongly influenced by the attractive forces. Other studies of the same systems have also shown that the lack of the attractive part of the potential is reflected more in the thermodynamics than the structure and that differences in their dynamics can be understood as a consequence of their thermodynamic differences [36]. In other respects, the influence of the intermolecular repulsion on dynamic and thermodynamic properties of model glass-forming mixtures have been studied by Coslovich and Roland [37], as well as by Shi *et al.* [38]. The authors modified the strength of repulsion by changing the repulsion exponent of the intermolecular potential and observed that potential softening has a negligible effect on the fragility and dynamic correlation volumes. Considering the briefly mentioned examples, one can conclude that the attractive term of the intermolecular potential has a significant impact on the feature of the supercooled liquids. However, the direct connection of the attractive forces and the tendency of the material to crystallization have not been elaborated yet. For that reason, in this paper, we focus on the above problem. To do that, we modify the standard LJ potential and subsequently, using CNT, we estimate the nucleation and crystal growth rates. The latter enable us to characterize the overall crystallization process and its dependence on the pressure in the case of different intermolecular attraction strength. Moreover, it is worth stressing that our modification of the intermolecular potential reflects that changes in the intermolecular interactions resulted from different values of the dipole moment and the polarizability for various molecules. Thus, our analysis can be directly compared with the experimental results obtained for the real systems.

II. METHODS

The standard LJ potential can be expressed in the following form:

$$V(r) = 4\varepsilon\left(\frac{\sigma}{r}\right)^{12} - 4\varepsilon\left(\frac{\sigma}{r}\right)^{6} \tag{1}$$

It consists of the repulsive $R(r) = 4\varepsilon\sigma^{12}/r^{12}$ and attractive $A(r) = -4\varepsilon\sigma^{6}/r^{6}$ potentials, the sum of which gives rise to the forces between molecules. Note that $A(r)$ originates from the short range interactions that take place between dipole-dipole, dipole-induced dipole, and London dispersion forces [39]. Thus, this term is directly related to the polarizability of the molecules and their dipole moments; hence, a proper set of the potential parameters can reflect differences in the strength of molecular interactions resulted from, e.g., solely different values of the dipole moment or polarizability. In this case, one should modify the attractive potential $A(r)$ and, at the same time, keep the repulsive potential $R(r)$ constant. Then, the values of the intermolecular potential parameters, i.e., ε and σ, should be chosen in this way to avoid modification of $R(r)$, while simultaneously to let $A(r)$ vary. Note that the described procedure above leads to a modification of the shape of the overall interaction potential $V(r)$, as well as to shift the position of its minimum and hence to a change of the ranges within which overall interactions are repulsive or attractive. Nevertheless, its great advantage is a direct relation to the real attractive interactions occurring between molecules. Therefore, we used this method to construct three different systems, which differ only in the strength of $A(r)$. The first of them is the standard one component LJ system with $\varepsilon = 1$ and $\sigma = 1$ ($V_{\mathrm{st}}(r) = R_{\mathrm{st}}(r) + A_{\mathrm{st}}(r)$). For the other two systems, we have chosen potential parameters in such a way that the terms, which parameterize attractive intermolecular interactions, are equal to $1.2 \cdot A_{\mathrm{st}}(r) = A_{1.2}(r)$ and $0.8 \cdot A_{\mathrm{st}}(r) = A_{0.8}(r)$,

whereas $R_{st}(r) = R_{1.2}(r) = R_{0.8}(r)$. Then, respective potential parameters are equal to $\varepsilon_{1.2} = 1.44$, $\varepsilon_{0.8} = 0.64$, $\sigma_{1.2} \approx 0.97$, and $\sigma_{0.8} \approx 1.04$. Note that potential parameters are expressed using GROMACS basic units [40], i.e., nanometer is a basic unit of length, whereas energy is specified by kilojoule per mole. Then, σ and ε, which are equal to 1 nm and 1 kJ/mol correspond to the standard LJ commonly described using the so-called LJ reduced units.

At the end of this section, we would like note that (as we already mentioned) the used technic of intermolecular potential modifications results in the changes of the values and shape of the overall interaction potential, which might cause the total attraction exerted on single molecule of the systems, defined as a sum of the attractive forces occurring between a given molecule and all other molecules of the system, to not necessarily increase in agreement with gain in $A(r)$. Therefore, using the following equation, $A_{\text{total}} = \int_{r_m}^{\infty} -4\pi r^2 \frac{dV}{dr} g(r) dr$, where $g(r)$ is the well-known radial distribution function (RDF), we estimate the average total attraction exerted on the single molecule of the systems, which indeed increases with enhancement of $A(r)$, i.e., A_{total} equals 12.7, 28.2, and 47.4 N/nm^2, respectively, for the system with the weakened, standard, and strengthened attraction part of the intermolecular potential. Hence, the method of intermolecular potential modifications, applied by us, is entirely justified in the context of the increase in intermolecular attraction.

III. RESULTS AND DISCUSSION

A. Determination of the melting point

The main goal of our research is to explore the effect of compression on the crystallization tendency of the systems characterized by different molecular attractions. Therefore, we have decided to consider the following three isobaric conditions, i.e., 10, 20, and 60 bars and the three attractive potentials $A_{0.8}(r)$, $A_{st}(r)$, and $A_{1.2}(r)$ (see Sec. II). The use of the CNT for our investigations requires, at the beginning, establishing the temperature dependences of the liquid and crystal volumes, as well as the melting temperatures for each examined systems at isobaric condition. To determine the mentioned dependencies, we generated perfect fcc crystal structure, which is well known as a stable crystal structure for the system described by LJ-like potentials. Subsequently, using the velocity Verlet algorithm with a time step equal to 0.001 ps, Nosé-Hoover thermostat, and Martyna-Tuckerman-Tobias-Klein barostat, we heated the system in the isothermal-isobaric *NPT* ensemble up to 40 K more than the sudden drop in the density of the system. At each temperature, to obtain reasonable results, we equilibrated the system for 500 000 time steps, and subsequently, we allocated another 500 000 time steps for data collecting. The examined systems contained 23 328 molecules weighing 1 u (basic GROMACS unit of mass). Since we study systems described by various potentials, we set a relatively large distance for the cutoff of intermolecular interactions, here, five times longer than the distance of the intermolecular potential minimum $r_c = 5 \cdot r_{\min} = 5 \cdot 2^{1/6}\sigma$. The latter ensures the sufficient minimization of the effects of different potential shifting for various systems. When the final temperature was reached, we subsequently cooled down systems to the starting

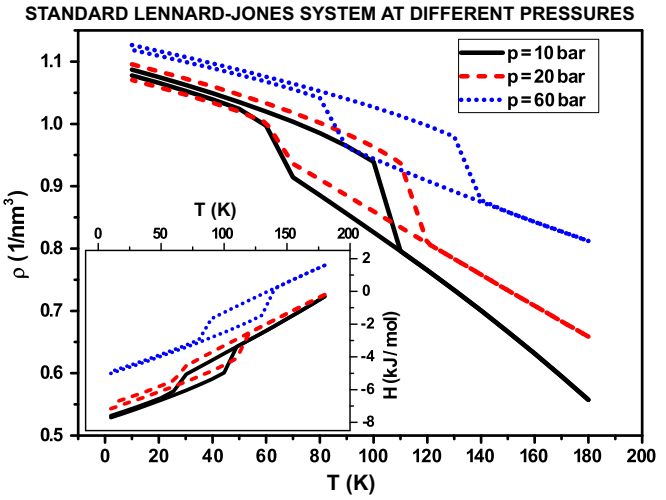

FIG. 1. Temperature dependence of the number density for standard LJ at different isobaric conditions. In the inset, the dependence of enthalpy on temperature for the same system is presented.

temperature. That procedure let us determine the temperature dependence of number density ρ and enthalpy H for crystal and liquid states (Fig. 1). For the purpose of further analysis, temperature dependencies $\rho(T)$ and $H(T)$ were approximated with an excellent accuracy by polynomial functions. In Fig. 1, one can easily observe the hysteresis between heating and cooling, which indicates the temperature range, within which the melting temperature is expected. However, maintenance of consistency between analyses of different systems at different pressures requires that the melting temperatures must be specified in a strictly defined way, which can be done by the use of the Raveché-Mountain-Streett (RMS) criterion [41]. According to this method, the melting temperature can be established as the temperature at which the ratio between the first nonzero minimum and the first maximum of the RDF is equal to 0.2+/−0.02. In Fig. 2, the RDF functions for different

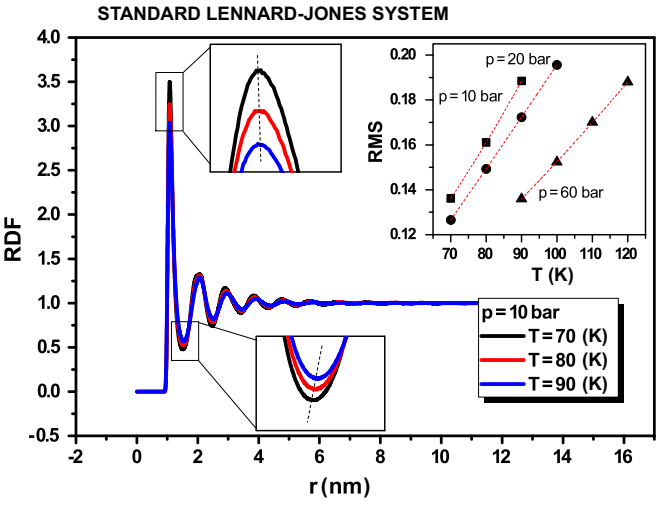

FIG. 2. The RDFs for standard LJ at different temperatures. In the inset, the value of the RMS criterion at different pressures and temperatures is presented.

temperatures at the pressure equal to 10 bars are presented for the standard LJ system, whereas, the temperature dependence of RMS values are shown in the inset of Fig. 2. As one can see, the temperature for which RMS values equal 0.2 is above the hysteresis temperature range; therefore, our results differ from the definition of RMS criterion, similar to results presented in Refs. [42,43]. However, we have checked the suggestion of Benjamin and Horbach [43], who have noted that RMS value at melting temperature is equal to 0.185. For that purpose, we have constructed the biphasic system (which is a connection of perfect fcc and liquid structures along a chosen direction) and performed the simulation at the suggested temperature in the *NPT* ensemble. At pressure equal to 10 and 20 bars, we did not observe any evidence of the melting or freezing for the LJ system. However, at pressure equal to 60 bars, the crystal structure of the biphasic LJ system melted, which implied that the estimated T_m was too high. Nevertheless, we observed that at the temperatures for which RMS criterion is equal to 0.175, all biphasic systems (also systems with the modified potentials) did not exhibit any tendency to melt or crystallization. Thus, we decided to define T_m as a temperature at which the RMS value is equal to 0.175 for all performed herein analysis. The time dependences of the biphasic system's volumes at the obtained melting temperatures are presented in the inset of Fig. 3(a). It can be seen that all biphasic systems indeed do not exhibit any trend to crystallization or melting. Thus, the estimated values of the melting temperature can be recognized as valid. Consequently, their pressure dependences are presented in the inset of Fig. 3(b) for all studied systems. We can observe that the increase of the molecular attraction strength causes the increase in the melting temperature, which can be easily explained by the fact that the stronger attractive forces make

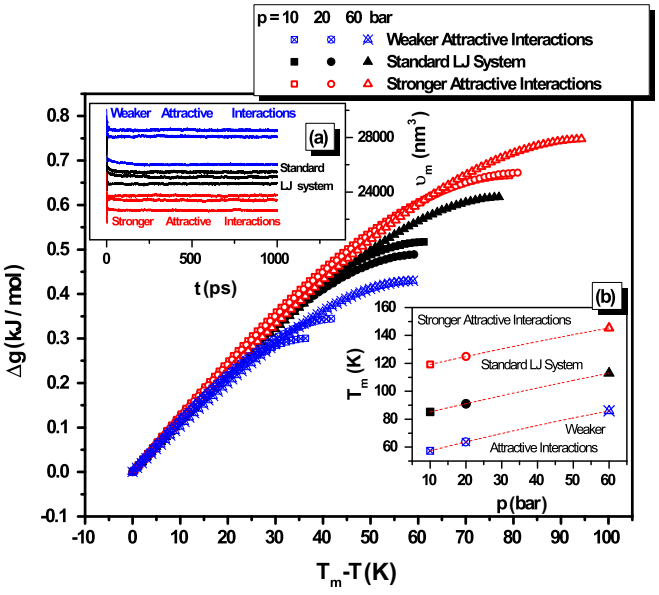

FIG. 3. Temperature dependence of the driving force for all studied systems. Inset (a) presents the time dependence of the biphasic system volumes at the melting temperature (determined from the value of RMS criterion equal to 0.175), whereas the dependence of the melting temperature on the pressure is presented in inset (b).

that crystal phase becomes more durable on thermal molecular motions, then more stable at higher temperatures. Interestingly, strengthening of the molecular attraction is reflected in values of T_m but not in its pressure dependence, i.e., the ratio dT/dp. Note that at the same thermodynamic conditions, the systems with stronger attraction forces occurring between molecules are denser and hence possess smaller values of the enthalpy.

B. Estimation of the nucleation barrier

As we already mentioned, the nucleation barrier depends on the two physical quantities, which are the driving force for crystallization and the interfacial free energy between solid and liquid states. These physical quantities, respectively, describe the tendency of a liquid to undergo the phase transformation and energy changes needed for the formation of a surface. In the case of homogeneous nucleation in spherical nuclei, the nucleation barrier, which is the work required for the formation of one critical nucleus, can be described by the following formula,

$$\Delta W = \frac{16}{3}\frac{\gamma^3}{(\Delta g)^2}. \tag{2}$$

The driving force has been calculated employing the standard integration method,

$$\Delta g = -\int_{T_m}^{T} \Delta S dT, \tag{3}$$

where ΔS is the difference of entropy between liquid and solid states. ΔS has been estimated by the well-known thermodynamic relationship $dS = dH/T$, using values of the enthalpy for both considered phases (see inset of Fig. 1, where $H(T)$ is shown for a standard LJ system). In Fig. 3, the temperature dependence of the driving force for crystallization is presented for each analyzed system. To unify our studies, which are performed for different systems at various thermodynamic conditions, we plot $\Delta g(T_m - T)$ instead of $\Delta g(T)$. From Fig. 3, it can be noticed that the first key quantity Δg achieves higher values for systems with enhanced molecular attraction, and the gain in Δg is most rapid for these systems.

The second key quantity controlling ΔW [see Eq. (2)] is the interfacial free energy between liquid and solid states. However, the measure of γ is a very challenging task, and special methods of computer simulations, unfortunately only applicable at the melting point, must be employed. In this paper, we use the CFM, which is described in detail in Refs. [23–25,44–48]. Therefore, herein, we present only a brief description. To apply this method, a special biphasic simulation box must be prepared. The plane of the interface must be located perpendicularly to the largest side of the simulation box and possess shape of an elongated rectangular, i.e., its width should be considerably longer than its height. The requisite shape of interface plane enables obtaining the quasi-one-dimensional function of the interface positions $h(y)$, where y is the coordinate in the direction along the interface. During the simulation run at the melting conditions, the interface positions fluctuate. The position fluctuations can be quantified at a discrete set of points, which represent capillaries. In the case of the quasi-one-dimensional interface, the amplitudes of capillary fluctuation modes relate to the

interfacial stiffness $\tilde{\gamma}_m$ by the following relation $\langle|h(q)|^2\rangle = k_B T_m / S\tilde{\gamma}_m q^2$, where $\langle\ldots\rangle$ represents the time average, k_B is the Boltzmann constant, S is the area of the interface, and $h(q)$ is the one-dimensional Fourier transformation of $h(y)$, with q as the wave number. From the above equation, the value of $\tilde{\gamma}_m$ can be easily obtained by plotting $\langle|h(q)|^2\rangle$ in a double logarithmic scale and subsequently fitting a linear function with constant slope equal to -2. Then, the interfacial stiffness can be extracted from the intercept of the fitting function. Note that $\tilde{\gamma}_m$ depends on the orientation of the crystal with respect to the interfacial plane, i.e., anisotropy. However, examinations of many model systems [23–25,49] and realistic molecular systems [44,50–52] suggest that this effect is usually relatively weak (of the order of few percent) and smaller than the uncertainties of the applied method. Therefore, in this paper, we identify $\tilde{\gamma}_m$ determined for a single (100) fcc orientation to the isotropic interfacial free energy $\tilde{\gamma}_m$.

Since our study requires use of a relatively large r_c and due to application of the periodic boundary conditions, imposing that r_c cannot be longer than the half of the shortest side of the simulation box, the constructed interfacial plane comprises 8×48 unit cells of the fcc shape. Consequently, the simulation box used for determination of γ_m contained 98 304 molecules separated evenly into liquid and solid phases. Initially, the crystal-melt biphasic systems were equilibrated for at least 100 000 time steps at the melting temperature in the *NPT* ensemble. Subsequently, we performed a comparatively long simulation run (1 000 000 time steps) during which the positions of molecules were stored every 500 time steps, which enables obtaining a reasonable statistic of the interface position fluctuations. However, it requires a distinction between liquid and solid particles. To do that, we calculate (for each molecule) the value of local order parameter defined in the following way: $\psi = |\frac{1}{N_{\vec{q}}}\frac{1}{Z}\sum_{\vec{r}}\sum_{\vec{q}}\exp(i\vec{q}\vec{r})|^2$, where $N_{\vec{q}}$ is the number of wave vectors $\vec{q}_i$ such that $\exp(i\vec{q}\vec{r}) = 1$ for any vector $\vec{r}$ connecting the Z neighbors in a perfect fcc lattice. The molecules were recognized as adjacent to the selected molecule if the distance between them was shorter than the double length of lattice constant. We omitted the antiparallel vectors; thus, $N_{\vec{q}}$ equal 6. Values of the local order parameter, defined in the way presented above, range from 0 to 1; values of ψ that are close to 0 are obtained for a totally disorder system, whereas $\psi = 1$ for the perfect fcc lattice. Since in any of analyzed configurations, atoms may occur that have a substantially different value from the local order parameter of their surroundings, we also averaged ψ over the neighboring values. Then, the particles can be classified as liquid or solidlike by a specified ψ value. In presented studies, molecules for which ψ achieves values higher than 0.5 are considered to belong to the solid phase. Finally, the position of the solid phase enables estimation of the interfacial fluctuations and hence determination of interfacial free energy between liquid and solid.

The obtained values of interfacial free energy at the melting condition γ_m are shown in Fig. 4. They are consistent with results obtained from the other studies using CFM [25], as well as different methods estimating γ_m [22,53]. In Fig. 4, one can see that the interactions with stronger attractive potential $A(r)$ result in higher values of γ_m. Moreover, the increase

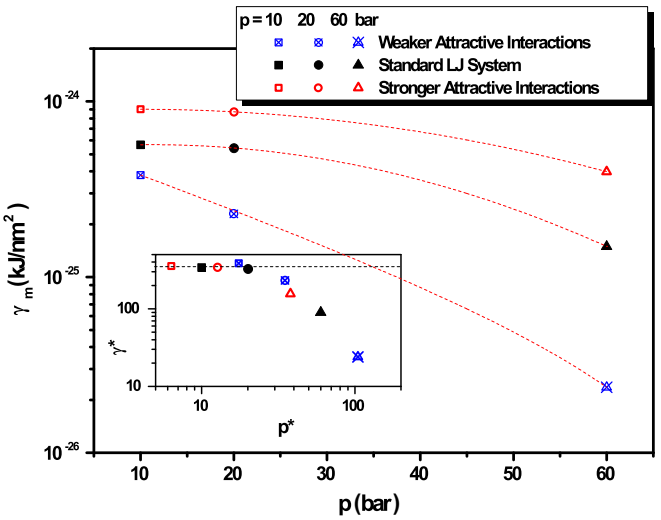

FIG. 4. Values of the interfacial free energy determined at the melting temperature using the CFM. The inset demonstrates interfacial free energy expressed in reduced simulation units. The dashed lines are a guide for the eye.

in pressure along the liquid-crystal coexistence line causes the decrease in γ_m for all examined systems. However, note that γ_m of systems with weaker attractive potential is more sensitive to pressure changes. Additionally, in the inset of Fig. 4, we present the values of interfacial free energies at the melting points in reduced LJ units γ_m^* as a function of reduced pressure p^*, which enables us to determine a common feature of γ_m for systems described by the LJ potential with exponents of repulsive $R(r)$ and attractive $A(r)$ potentials equal to 12 and 6, respectively. At p^* equals ~20, one may observe that the pressure dependence of γ_m^* changes from almost invariant to a decreasing one. However, the disclosure of a reason of noted change of interfacial free energy at melting conditions in LJ-like systems requires further studies. It must also be taken into account that orientation of the crystal structure concerning the interface plane influences the behavior of $\gamma_m(p_m)$ [28]. In our studies, we consider (100) orientation of the crystal, for which, similar to Ref. [28], γ_m decreases with the temperature at the melting conditions.

Both the lowering of the γ_m when the pressure (and temperature) is increasing and the gain in γ_m with the increase in molecular attraction can be explained using the Spaepen [54] approach to the interfacial free energy between liquid and solid. Based on those ideas, the excess free energy, which emerges due to the presence of the solid-liquid interface, is caused by the difference in configurational entropy between bulk and interface liquid molecules. The configurational entropy for liquid molecules of the interface is smaller than for liquid molecules of bulk because solids molecules of the interface reduce the number of available configurations for liquid molecules of the interface. Consequently, the difference in configurational entropy between liquid and solid molecules of the interface $\Delta S_{\mathrm{conf}}^{\mathrm{interface}}$ is smaller than the respective difference for bulk liquid $\Delta S_{\mathrm{conf}}^{\mathrm{bulk}}$. The arising difference $\Delta S_{\mathrm{conf}}^{\mathrm{bulk}} - \Delta S_{\mathrm{conf}}^{\mathrm{interface}}$ should be compensated by the respective interfacial free energy. Hence, the dependence of the configurational entropies

for bulk and interface is responsible for the behavior of γ (also at the melting conditions). The configurational entropies can be reduced by the repulsive intermolecular interactions, which lessen the number of possible configurations. Then, to explain the observed decrease in γ_m triggered by compression, as well as by the increase in molecular attraction, we should determine whether interactions between molecules at the melting conditions are attractive or repulsive. It can be done by estimation of the average distance between molecules in the liquid state at melting conditions $d_0 = \rho_l^{-1/3}$, where ρ_l is the number density of the liquid. In Fig. 5(a), we can see that obtained for all examined systems, values of d_0 are smaller than the distance at which the respective potentials possess minimum r_m (to clarify the presentation of the results, we decided to present in Fig. 5 solely outcomes for two extreme systems). Taking into account that r_m defines the distance between molecules at which repulsive and attractive forces cancel each other, we can see that LJ interactions occurring between molecules of the supercooled liquid and solid are repulsive [55–62]; hence, gain in the intermolecular forces reduces configurational entropies for molecules of the bulk and interface. Considering the effect of compression on a chosen system, one can see in Fig. 5(b) that the intermolecular forces become stronger when the pressure increases, which results in the abovementioned reduction of the configurational entropies. However, the effect of compression on configurational entropy is not identical for the molecules of the bulk and interface, i.e., it is less pronounced at the interface because of the presence of solid molecules, which are less susceptible on compression then the liquid molecules. Thus, the compression of the system implies the reduction of $\Delta S_{\mathrm{conf}}^{\mathrm{bulk}}$ and $\Delta S_{\mathrm{conf}}^{\mathrm{interface}}$, wherein $\Delta S_{\mathrm{conf}}^{\mathrm{bulk}}$ decreases more. Consequently, $\Delta S_{\mathrm{conf}}^{\mathrm{bulk}} - \Delta S_{\mathrm{conf}}^{\mathrm{interface}}$ decreases with compression, making γ_m a decreasing function of the pressure.

In the second case presented in Fig. 4, i.e., in the case of attractive intermolecular potential influence on the interfacial free energy, we stress that the different systems are compared. Therefore, comparison between absolute values of physical quantities or between their absolute changes might be not sufficient to obtain valid conclusions, because of the various influence of a given change of the specific physical quantity, e.g., the strength of the intermolecular forces occurring between molecules, on the modification of other physical quantities (configurational entropy) for different systems. This problem can be overcome by scaling of the studied properties, which enables comparison of the relative values of physical properties. One of the possible ways to perform the above analysis is consideration of values of force and length expressed in the reduced LJ units $F^* = F\sigma/\varepsilon$ and $d_0^* = d_0/\sigma$. In Fig. 5(c), one can see that at isobaric conditions (denoted by the same geometric figure, i.e., square, circle, and triangle, represent 10, 20, and 60 bars, respectively), F^* is higher for the system with the weaker attractive intermolecular interactions. Thus, at constant pressure, molecules with weaker attraction exert smaller forces on their neighbors F [presented in Fig. 5(b)], but, in fact, they possess stronger relative impact on them (because of the thermodynamic properties of the system). This implies that the molecule of the system with the weaker attractive intermolecular potential more substantially reduced the configurational entropy of the surrounding. Hence, the

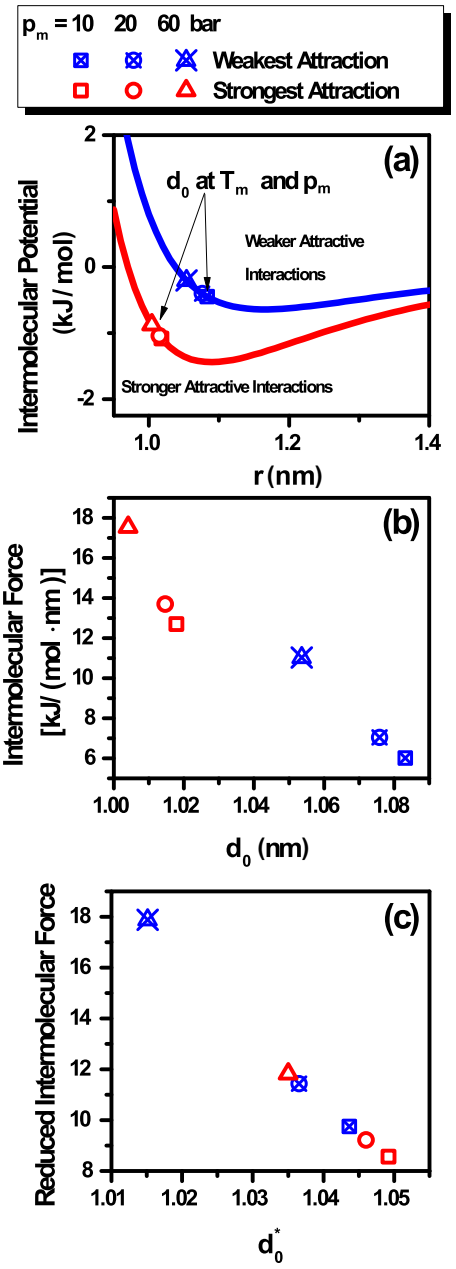

FIG. 5. In (a), the overall intermolecular potential curves for two extreme systems, i.e., for systems with the strongest and weakest attractive potential, are presented. The points denote values of the potential determined at the average distance for the liquid states at melting conditions d_0; (b) shows values of the forces occurring between molecules at the melting conditions as a function d_0, whereas the same dependence expressed in the reduced LJ units is presented in (c).

system characterized by the weakest attractive intermolecular potential possesses the smallest values of the configurational entropies, implying the tiniest values of $\Delta S_{\mathrm{conf}}^{\mathrm{bulk}} - \Delta S_{\mathrm{conf}}^{\mathrm{interface}} \sim \gamma$. Consequently, we observe in Fig. 4 that γ_m is an increasing function of the attractive intermolecular potential at the isobaric conditions. In Fig. 5(c), we can also see that the increase in the forces occurring between molecules induced by the increase in the pressure is the highest for the system with the weakest attractive intermolecular potential. As explained

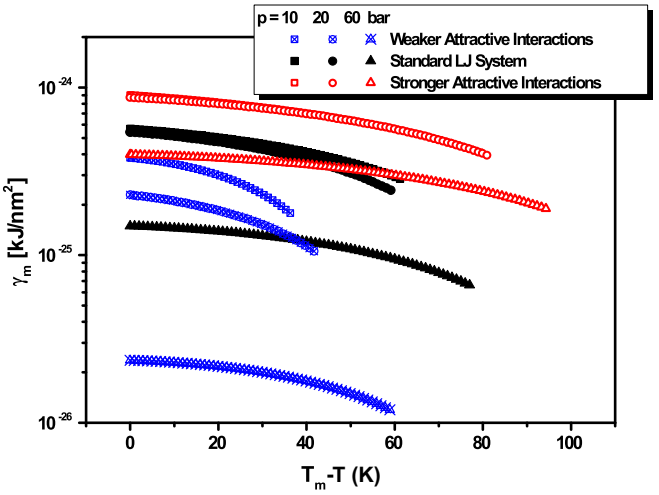

FIG. 6. Predicted results by the modified Turnbull law dependencies of the interfacial free energy on temperature expressed as a function of the difference between melting temperature and the temperature.

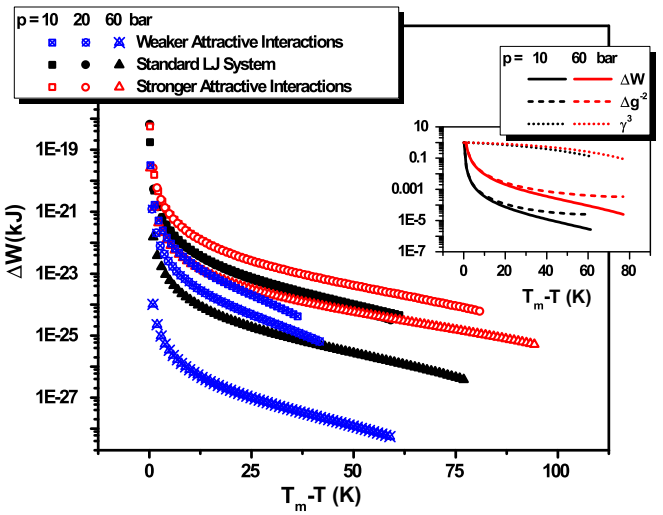

FIG. 7. The temperature dependences of the nucleation barriers for studied systems. In the inset, the temperature dependence of the normalized values of ΔW, Δg^{-2}, and γ^3 at pressures equal to 10 and 60 bars for standard LJ system are presented.

above and observed in Fig. 4, the drop in γ_m due to compression is most evident for the system characterized by the weakest attractive potential.

Since in this paper we focus on the study of the tendency to crystallization from the liquid state at various isobaric conditions, which is usually observed below the melting point, it is necessary to establish the temperature dependence of the interfacial free energy. In this context, note that there are number of papers presenting studies based on molecular dynamic simulations in which some effective $\gamma(T)$ are used to reproduce nucleation rate in the framework of CNT [63–67]. In those papers, authors consider the increasing dependence of γ on T, which can be explained by the entropy loss due to the ordering of the liquid near the interface [68]. Taking the above into account, we use $\gamma(T)$ in the form of the modified Turnbull law suggested in Ref. [64] $\gamma(T) = \gamma_m[\frac{\rho_c(T)}{\rho_c(T_m)}]^{2/3}[\frac{\Delta H(T)}{\Delta H(T_m)}]$, where ρ_c is the number density of the crystal phase and ΔH is the difference of enthalpy between the crystal and the liquid at the given temperature T. The predicted results by the modified Turnbull law dependencies of γ on T are presented in Fig. 6 as a function of $T_m - T$. According to that which we mentioned in the Introduction, the interfacial free energy should lower upon cooling and should be accompanied by the growth of the driving force for crystallization. Indeed, from Eq. (2), both effects should combine and make that the nucleation barrier becomes smaller. In fact, Fig. 7 clearly shows a drop in ΔW during cooling. Note that the system characterized by the weakest intermolecular attractive potential $A(r)$ exhibits thermodynamic features, which foster crystallization the most, i.e., it possess the smallest value of ΔW. Furthermore, for that system, $\Delta W(T)$ decreases most after compression. Even a slight increase in pressure is reflected in noticeable changes of the nucleation barrier, which is not observed for the systems with the strongest intermolecular attractive potentials ($\Delta W(T)$ at pressures equal to 10 and 20 bars are not distinguishable for that system). The scenario described is consistent with results in Fig. 6, because values of $\gamma(T)$, which are smaller for the system with weaker intermolecular attractive potential, have the most variation for that system. Linking this observation with almost identical $\Delta g(T)$ for all studied systems (see Fig. 3), we can suppose that the interfacial free energy between liquid and solid states is mainly responsible for the observed influence of intermolecular attractive potential on ΔW values. However, plotting normalized values of $\Delta W_{\mathrm{norm}}(T) = \Delta W(T)/\Delta W_{\mathrm{max}}$, $\Delta g^{-2}_{\mathrm{norm}} = \Delta g^{-2}(T)/\Delta g^{-2}_{\mathrm{max}}$, and $\gamma^3_{\mathrm{norm}}(T) = \gamma^3(T)/\gamma^3_{\mathrm{max}}$ [according to Eq. (2)], one can see that the dependence of the nucleation barrier, i.e., its change during cooling, is mostly affected by the behavior of the $\Delta g(T)$; see the inset of Fig. 7, where data for the standard LJ system at 10 and 60 bars are presented.

C. Rates of nucleation, crystal growth, and overall crystallization

So far, we only considered the influence of the pressure on thermodynamic properties of the examined systems. However, molecular mobility also plays an important role in nucleus creation. Increased liquid viscosity retards diffusion of molecules and impedes nucleation. Therefore, during cooling, dynamics of the molecules affects the crystallization in the opposite way than thermodynamics. Hence, the interplay between kinetic and thermodynamic factors determines the outcome of the crystallization process. The CNT takes into account both mentioned influences. According to CNT, beside ΔW diffusion, D is the important parameter controlling nucleation. Then, the steady-state nucleation rate J can be estimated from the expression

$$J = \rho_l^{4/3}\sqrt{\frac{\gamma}{k_B T}}\, D \exp\left(-\frac{\Delta W}{k_B T}\right), \tag{4}$$

where ρ_l is the number density of the liquid. In this paper, the diffusion coefficient has been estimated from the long-term evolution of the mean square displacement calculated at different temperatures in the liquid state. For temperatures lower than the melting temperature, D has been obtained by

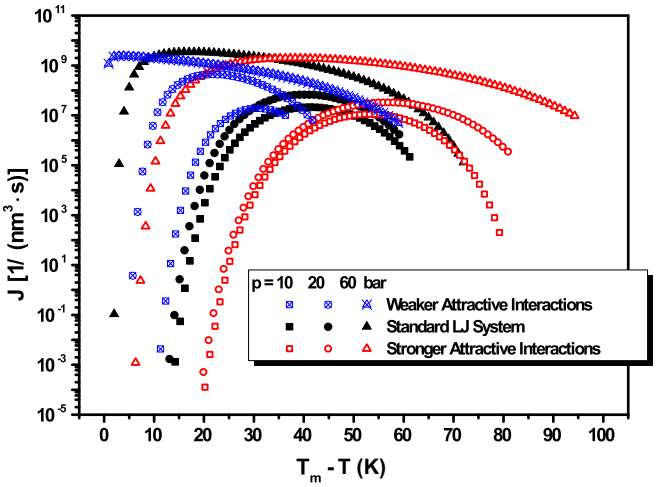

FIG. 8. Temperature dependence of the nucleation rates estimated according to CNT for the analyzed systems.

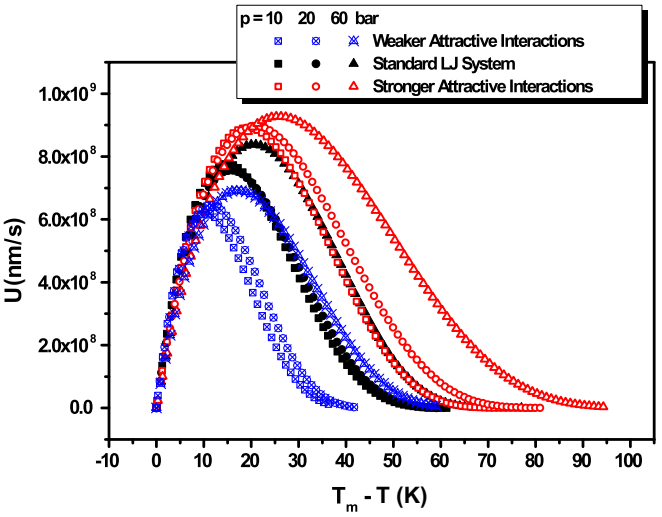

FIG. 9. Temperature dependence of the crystal growth rates estimated according to CNT for the analyzed systems.

approximation of the $D(T)$ dependence for liquid by the Vogel-Fulcher-Tammann equation [69–71].

Note that many tests of the CNT validity have been reported in the literature. Thus, the obtained results are not unequivocal because agreement, as well as disagreement, between predictions of nucleation rate according to CNT and the rates experimentally measured or directly determined from simulations [72] have been reported. In most cases, noted differences result from discrepancies in the kinetic pre-exponential factor occurring in Eq. (4) [68]. For example, according to Ref. [73], the kinetic pre-exponential factor obtained in the simulation of the LJ system is about two orders of magnitude larger than the one predicted by CNT, leading to larger value of the nucleation rate. However, despite the mentioned problems, the simplicity of CNT makes this theory frequently exploited to explain crystal nucleation in simulations and experiments. The calculated values of nucleation rates for the studied systems are presented in Fig. 6. Similar to the previous simulations and experimental results, the increase in pressure implies the acceleration of the nucleation. Moreover, in Fig. 8, it can be seen that the weaker attraction is reflected in the higher values of J close to the melting temperature. Thus, increase in molecular attraction generates difficulties in the creation of a critical nucleus, which implies better glass-forming ability of a given system. From Fig. 8, one can also notice that the strength of intermolecular attraction is reflected in the changes of nucleation rate, i.e., the system with the weakest attractive intermolecular potentials exhibits a significant gain in J during compression from 10 to 20 bars, which is not observed for other systems. For the latter, the substantial gain in J occurs after increasing p up to 60 bars. Note that for those systems, γ_m (Fig. 4) exhibits a noticeable decrease in the discussed pressure range.

The CNT predicts that after formation of the critical nucleus, the crystal phase grows within the bulk liquid. The rate of the crystal expansion is parameterized by the crystal growth,

$$U = f\frac{D}{4}\rho^{1/3}\left[1 - \exp\left(\frac{\Delta g}{k_B T}\right)\right], \tag{5}$$

where f is a parameter that has different values for various modes of growth. In our paper, we assume that it is equal to unity for all analyzed systems. In Fig. 9, it can be seen that U becomes higher when the strength of molecular attraction increases. Moreover, the compression causes the maxima of crystal growth to shift toward the lower temperatures. However, the above effect is similar for all systems, and we do not observe any characteristic influence of molecular attraction on crystal growth. Nevertheless, combining results presented in Figs. 8 and 9, one may note that the curves of nucleation rate and crystal growth are closer to each other for the system with the weakest molecular attractive potential than for other systems. The temperature range between $J_{\max}$ and $U_{\max}$ is about 15 K (at $p = 10$ bars), whereas at the analyzed isobaric conditions, the discussed distances equal about 25 and 35 K, respectively, for the standard LJ system and the system with enhanced molecular attractive potential. The small separation between nucleation and crystal growth implies that the crystallization proceeds easily because the formation of nuclei is promptly supported by their growth. The combined effect of J and U are considered by CNT as a rate of overall crystallization and can be expressed by the following formula

$$k = \tfrac{1}{3}\pi U^3 J, \tag{6}$$

which parameterizes progress of crystallization in the unit of time. In Fig. 10, we present the calculated values of the overall crystallization rate for the studied systems. One can observe that molecular attraction does not significantly influence the rate of overall crystallization but rather its temperature range. We can also see that the systems with different attractive potentials exhibit the various behaviors of overall crystallization rate during the compression. When the pressure increases from 10 to 20 bars, the most significant increase in k is observed for the system with the weakest molecular attractive potential. For other systems, compression from 10 to 20 bars does not exert such great influence on overall crystallization rate. However, for those systems, the gain in pressure from 20 to 60 bars causes much larger acceleration in the crystallization process. Thus, we may

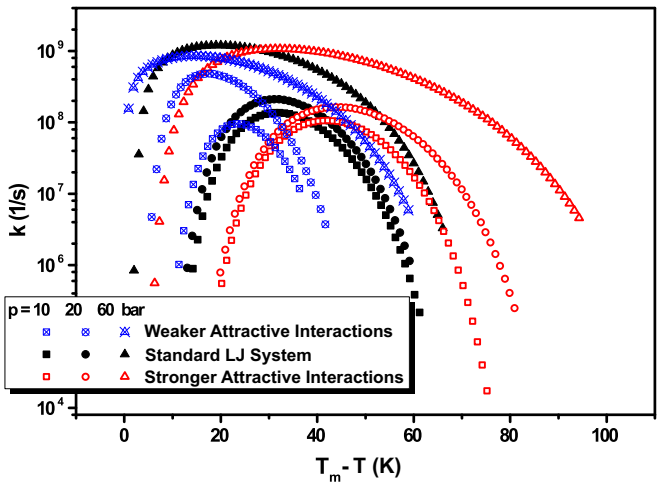

FIG. 10. Temperature dependence of the overall crystallization rates estimated according to CNT for the analyzed systems.

conclude that molecular attraction influences the separation of the nucleation and crystal growth processes, as well as the pressure range at which overall crystallization is significantly facilitated. We want to focus the reader's attention on another interesting result displayed in Fig. 10. For the system with the strongest molecular attraction, compression from 10 to 20 bars moves the maximum of k toward the lower temperature, whereas the increase in pressure for a further 40 bars results in the maximum displacement in the opposite direction. This is not observed for a standard LJ system and the system with weakened molecular attractive potential. The inconsistent shift of the overall crystallization rate during compression can possess two possible origins. The discussed result may be a mutual feature of LJ-like systems, which is observed in the pressure ranges depending on the strength of intermolecular interactions, or the strengthening of the attractive potential between molecules above some value causes the observed manner of maxima. Nevertheless, irrespective of causes of the $k^{\max}(T)$ behavior, the gain in p always results in the increase of k at the constant distance from the melting temperature.

IV. CONCLUSIONS

In this paper, we have examined, in terms of CNT, how the strengthening of the attractive term of the intermolecular potential influences the crystallization process for the LJ-like systems at different isobaric conditions. We did not observe any significant variation in the behavior of the melting temperature or in the values of the driving force during compression of the studied systems. However, the interesting result has been noted for the interfacial free energy on the liquid-crystal coexistence line. The decrease of γ_m, which is due to compression on the coexistence curve, becomes more substantial when the strength of attractive potential decreases. The pressure behavior of γ_m could be explained in terms of Spaepen's definition of γ, which involves differences between configurational entropies for bulk and interface as key quantities determining values of γ. The increase in pressure makes that the average distance between molecules decreases, and as we presented, the forces occurring between molecules become stronger. The configurational entropies are reduced, and consequently the interfacial free energy decreases. Our study also revealed that the enhancement of the attractive potential, similar to the compression, makes the forces occurring between molecules stronger, causing, paradoxically, the increase in the interfacial free energy. However, disclosing the influence of the molecular attraction on the interfacial free energy was more complex because the comparisons between different systems, which are certainly systems with modified interaction potential, require an application of some scaling. Calculation of the reduced values of the intermolecular forces reveals that the system with the weakest molecular attraction exhibits the highest values of the reduced (relative) forces. It explains the observed and, at first glance, the paradoxical increase of the interfacial free energy induced by the strengthening of the intermolecular attraction, as well as the most noticeable effect of compression on γ_m for the system with the weakest attractive potential. The presented dependence of γ_m on molecular attraction is reflected in values of the nucleation barriers for the formation of the critical nucleus, which are smaller when the molecular attraction is weaker. Consequently, both nucleation rate and overall crystallization rate exhibit visible changes caused by the various strength of attractive intermolecular potential, whereas crystal growth, in which interfacial free energy does not play any role, is less affected by modification of intermolecular potential. To summarize, we can suspect that modification in the intermolecular potential mainly influences the values of the liquid-crystal interface. However, we should stress that the LJ is an exclusive model system and results obtained for it may differ from the ones obtained for the real systems. Nevertheless, we are deeply hopeful that our research will stimulate experimenters to verify of our outcomes. However, detailed experimental investigation of the mechanism, which governs the relationship, requires consideration of another fascinating aspect that arises, i.e., the anisotropy of the molecules.

ACKNOWLEDGMENTS

Part of this work received funding from the Interreg 2 Seas Program 2014–2020, cofunded by the European Regional Development Fund under the Innovative Multicomponent Drug Design (IMODE) Project. Moreover, K.A., K.K., and M.P. are grateful for the financial support from the National Science Centre within the framework of the Opus project (Grant No. DEC 2014/15/B/ST3/00364).

[1] L. Yu, Adv. Drug Delivery Rev. **48**, 27 (2001).
[2] M. D. Demetriou, M. E. Launey, G. Garrett, J. P. Schramm, D. C. Hofmann, W. L. Johnson, and R. O. Ritchie, Nat. Mater. **10**, 123 (2011).
[3] A. S. Myerson, *Handbook of Industrial Crystallization,* 2nd ed. (Butterworth-Heinemann, Woburn, MA, 2002).
[4] L. Novoa, J. J. Braga, and D. Addadi, *Engineering of Crystalline Materials Properties: State of the Art in Modeling, Design and Applications* (Springer, Dordrecht, The Netherlands, 2008).
[5] P. G. Debenedetti, *Metastable Liquids Concepts and Principles* (Princeton University Press, Princeton, NJ, 1996).

[6] G. Tammann, *Aggregatzustände : die Zustandsänderungen der Materie in Abhängigkeit von Druck und Temperatur* (Leopold Voss Verlag, Leipzig, 1922).
[7] M. Hasselblatt, Z. Anorg. Allg. Chem. **119**, 325 (1921).
[8] M. Hasselblatt, Z. Anorg. Allg. Chem. **119**, 353 (1921).
[9] N. N. Sirota, *Crystallization and Phase Transformations* (Academy of Sciences of Belorussian SSR, Minsk, 1962).
[10] D. R. Uhlmann, J. F. Hays, and D. Turnbull, Phys. Chem. Glasses **7**, 159 (1966).
[11] M. J. Aziz, E. Nygren, J. F. Hays, and D. Turnbull, J. Appl. Phys. **57**, 2233 (1985).
[12] T. Yoshino, K. Maruyama, H. Kagi, M. Nara, and J. C. Kim, Cryst. Growth Des. **12**, 3357 (2012).
[13] C. H. Polsky, L. M. Martinez, K. Leinenweber, M. A. VerHelst, C. A. Angell, and G. H. Wolf, Phys. Rev. B **61**, 5934 (2000).
[14] K. Adrjanowicz, K. Kaminski, Z. Wojnarowska, M. Dulski, L. Hawelek, S. Pawlus, M. Paluch, and W. Sawicki, J. Phys. Chem. B **114**, 6579 (2010).
[15] R. B. Dow, J. Chem. Phys. **7**, 201 (1939).
[16] M. Mierzwa, M. Paluch, S. J. Rzoska, and J. Zioło, J. Phys. Chem. B **112**, 10383 (2008).
[17] U. Köncke, H. G. Zachmann, and F. J. Baltá-Calleja, Macromolecules **29**, 6019 (1996).
[18] J. Zhang, D.-X. Yan, J.-Z. Xu, H.-D. Huang, J. Lei, and Z.-M. Li, AIP Adv. **2**, 042159 (2012).
[19] K. Koperwas, K. Adrjanowicz, Z. Wojnarowska, A. Jedrzejowska, J. Knapik, and M. Paluch, Sci. Rep. **6**, 36934 (2016).
[20] J. Q. Broughton and G. H. Gilmer, J. Chem. Phys. **79**, 5119 (1983).
[21] R. L. Davidchack and B. B. Laird, Phys. Rev. Lett. **85**, 4751 (2000).
[22] R. L. Davidchack and B. B. Laird, J. Chem. Phys. **118**, 7651 (2003).
[23] J. J. Hoyt, M. Asta, and A. Karma, Phys. Rev. Lett. **86**, 5530 (2001).
[24] J. R. Morris, Phys. Rev. B **66**, 144104 (2002).
[25] J. R. Morris and X. Song, J. Chem. Phys. **119**, 3920 (2003).
[26] Y. Mu, A. Houk, and X. Song, J. Phys. Chem. B **109**, 6500 (2005).
[27] T. Frolov and Y. Mishin, J. Chem. Phys. **131**, 054702 (2009).
[28] B. B. Laird, R. L. Davidchack, Y. Yang, and M. Asta, J. Chem. Phys. **131**, 114110 (2009).
[29] J. W. P. Schmelzer, *Glass: Selected Properties and Crystallization* (Walter de Gruyter, Berlin, 2014).
[30] A. Rahman, Phys. Rev. **136**, A405 (1964).
[31] J. R. Morris, U. Dahlborg, and M. Calvo-Dahlborg, J. Non.-Cryst. Solids **353**, 3444 (2007).
[32] C. De Michele, F. Sciortino, and A. Coniglio, J. Phys.: Condens. Matter **16**, L489 (2004).
[33] S. Sengupta, F. Vasconcelos, F. Affouard, and S. Sastry, J. Chem. Phys. **135**, 194503 (2011).
[34] J. Gerges, Ph.D. thesis, University of Lille, 2016.
[35] L. Berthier and G. Tarjus, Phys. Rev. Lett. **103**, 170601 (2009).
[36] A. Banerjee, S. Sengupta, S. Sastry, and S. M. Bhattacharyya, Phys. Rev. Lett. **113**, 225701 (2014).
[37] D. Coslovich and C. M. Roland, J. Non.-Cryst. Solids **357**, 397 (2011).
[38] Z. Shi, P. G. Debenedetti, F. H. Stillinger, and P. Ginart, J. Chem. Phys. **135**, 084513 (2011).
[39] P. Atkins and J. de Paula, in *Atkins' Physical Chemistry* (Oxford University Press, Oxford, United Kingdom, 2014), pp. 659–696.
[40] GROMACS Development Teams, GROMACS Reference Manual, Version 5.1. Royal Institute of Technology and Uppsala University, Sweden, ftp://ftp.gromacs.org/pub/manual/manual-5.1-beta1.pdf (accessed 8 Sep. 2016).
[41] H. J. Raveché, R. D. Mountain, and W. B. Streett, J. Chem. Phys. **61**, 1970 (1974).
[42] A. Ahmed and R. J. Sadus, Phys. Rev. E **80**, 061101 (2009).
[43] R. Benjamin and J. Horbach, J. Chem. Phys. **143**, 014702 (2015).
[44] X. Feng and B. B. Laird, J. Chem. Phys. **124**, 044707 (2006).
[45] J. J. Hoyt and M. Asta, Phys. Rev. B **65**, 214106 (2002).
[46] J. R. Morris and R. E. Napolitano, JOM **56**, 40 (2004).
[47] A. A. Potter and J. J. Hoyt, J. Cryst. Growth **327**, 227 (2011).
[48] R. L. Davidchack, J. R. Morris, and B. B. Laird, J. Chem. Phys. **125**, 094710 (2006).
[49] M. Amini and B. B. Laird, Phys. Rev. B **78**, 144112 (2008).
[50] J. Benet, L. G. MacDowell, and E. Sanz, Phys. Chem. Chem. Phys. **16**, 22159 (2014).
[51] R. L. Davidchack, R. Handel, J. Anwar, and A. V. Brukhno, J. Chem. Theory Comput. **8**, 2383 (2012).
[52] R. Handel, R. L. Davidchack, J. Anwar, and A. Brukhno, Phys. Rev. Lett. **100**, 036104 (2008).
[53] X. M. Bai and M. Li, J. Chem. Phys. **124**, 124707 (2006).
[54] F. Spaepen, Acta Metall. **23**, 729 (1975).
[55] J. D. Weeks, D. Chandler, and H. C. Andersen, J. Chem. Phys. **54**, 5237 (1971).
[56] U. R. Pedersen, N. P. Bailey, T. B. Schrøder, and J. C. Dyre, Phys. Rev. Lett. **100**, 015701 (2008).
[57] N. P. Bailey, U. R. Pedersen, N. Gnan, T. B. Schrøder, and J. C. Dyre, J. Chem. Phys. **129**, 184507 (2008).
[58] N. P. Bailey, U. R. Pedersen, N. Gnan, T. B. Schrøder, and J. C. Dyre, J. Chem. Phys. **129**, 184508 (2008).
[59] D. Coslovich and C. M. Roland, J. Phys. Chem. B **112**, 1329 (2008).
[60] D. Coslovich and C. M. Roland, J. Chem. Phys. **130**, 014508 (2009).
[61] T. B. Schrøder, U. R. Pedersen, N. P. Bailey, S. Toxvaerd, and J. C. Dyre, Phys. Rev. E **80**, 041502 (2009).
[62] A. Grzybowski, K. Koperwas, and M. Paluch, Phys. Rev. E **86**, 031501 (2011).
[63] L. J. Peng, J. R. Morris, and R. S. Aga, J. Chem. Phys. **133**, 084505 (2010).
[64] R. S. Aga, J. R. Morris, J. J. Hoyt, and M. Mendelev, Phys. Rev. Lett. **96**, 245701 (2006).
[65] V. G. Baidakov, S. P. Protsenko, and A. O. Tipeev, J. Chem. Phys. **139**, 224703 (2013).
[66] S. R. Wilson and M. I. Mendelev, Model. Simul. Mater. Sci. Eng. **22**, 065004 (2014).

[67] K. F. Kelton and A. L. Greer, *Nucleation in Condensed Matter* (Elsevier, New York, 2010).
[68] D. T. Wu, L. Gránásy, and F. Spaepen, MRS Bull. **29**, 945 (2004).
[69] H. Vogel, Phys. Z. **22**, 645 (1921).
[70] G. S. Fulcher, J. Am. Ceram. Soc. **8**, 339 (1925).
[71] G. Tammann and W. Hesse, Z. Anorg. Allg. Chem. **156**, 245 (1926).
[72] K. F. Kelton, in *Solid State Physics*, edited by H. Ehrenreich and D. Turnbull (Elsevier B.V., New York, 1991), pp. 75–177.
[73] P. Rein ten Wolde, M. J. Ruiz-Montero, and D. Frenkel, J. Chem. Phys. **104**, 9932 (1996).